# Energy-Transfer Modeling for the Rational Design of Multiporphyrin Light-Harvesting Arrays

**P. Gregory Van Patten,[†] Andrew P. Shreve,[†] Jonathan S. Lindsey,*[,‡] and Robert J. Donohoe*[,†]**

*Biochemistry and Biotechnology Group, CST-4, MS J586, Los Alamos National Laboratory, Los Alamos, New Mexico 87545, and Department of Chemistry, North Carolina State University, Raleigh, North Carolina 27695-8204*

*Received: July 15, 1997; In Final Form: February 18, 1998*

Excited-state energy migration among a collection of pigments forms the basis for natural light-harvesting processes and synthetic molecular photonic devices. The rational design of efficient energy-transfer devices requires the ability to analyze the expected performance characteristics of target molecular architectures comprised of various pigments. Toward that goal, we present a general tool for modeling the kinetics of energy migration in weakly coupled multipigment arrays. A matrix-formulated eigenvalue/eigenvector approach has been implemented, using empirical data from a small set of prototypical molecules, to predict the quantum efficiency (QE) of energy migration in a variety of arrays as a function of rate, competitive processes, and architecture. Trends in the results point to useful design strategies including the following: (1) The QE for energy transfer to a terminal acceptor upon random excitation within a linear array of isoenergetic pigments decreases rapidly as the length of the array is increased. (2) Increasing the rate of transfer and/or the lifetime of the competitive deactivation processes significantly improves QE. (3) Qualitatively similar results are obtained in simulations of linear molecular photonic wires in which excitation and trapping occur at opposite ends of the array. (4) Branched and cyclic array architectures exhibit higher QEs than linear architectures with equal numbers of pigments. (5) Dramatic improvements in QE are achieved when energy transfer is directed by a progressive downward cascade in excited-state energy. (6) The most effective light-harvesting architectures are those where isolated pools of donors each have independent paths directly to the terminal acceptor. Collectively, these results provide valuable insight into the types of molecular designs that are expected to exhibit high efficiency in overall energy transfer.

## Introduction

Self-assembled aggregates and covalently linked arrays of metalloporphyrins provide the basis for molecular photonic devices and biomimetic light-harvesting systems.[1−9] Numerous oligomeric porphyrinic arrays have been synthesized with the goal of optimizing photophysical properties, including absorption cross-section and directed energy-transfer reactions. The absorption properties of these model systems can often be predicted on the basis of the spectra of the component pigments, but the overall efficiency of energy transfer in large arrays is much more difficult to anticipate, even if the efficiencies are known for individual energy-transfer steps. Because the synthesis of large arrays is a time- and materials-intensive process, the ability to reliably predict the properties of target complexes is highly desirable.

The methodology for preparing synthetic porphyrin-containing light-harvesting arrays has advanced significantly, and now many different architectures can be accessed. Osuka has prepared a linear porphyrin array containing nine porphyrins,[10] Sanders has pioneered the synthesis of cyclic arrays containing up to five porphyrins,[11,12] and numerous strategies have emerged for preparing arrays of various geometries containing five to nine porphyrins.[13−23] Moore has prepared a dendrimeric structure comprised of a cascade of arylethynyl chromophores.[24] Self-assembling architectures comprised of porphyrinic pigments[25−30] or metal coordination complexes[31] also have been developed. We have synthesized soluble multiporphyrin arrays incorporating a diarylethyne linkage that establishes a relatively fixed inter-porphyrin distance (∼20 Å center-to-center).[13−15,32] As examples, a star-shaped pentameric array functions as an energy funnel (Figure 1A), while a linear array of five pigments transfers excited-state energy from one end to the other and constitutes a molecular photonic wire (Figure 1B).[33] Variants of this latter architecture function as optoelectronic gates.[34]

These advances in synthetic capabilities now enable explicit consideration of design issues such as architecture, numbers of pigments, pigment properties (spectral, electronic), interconnections, and energy gradients. Because of this diversity of choices, computational tools are of critical importance for evaluating the designs of possible light-harvesting systems and molecular photonic devices. Arrays comprised of weakly coupled pigments are ideally suited for energy-transfer modeling, as the energy-transfer process occurs without significant alteration of the remaining excited-state photophysical processes. Consequently, energy-transfer rates can be considered independently of the intrinsic electronic structures of the individual pigments. (In contrast, strong coupling generally results in a new supermolecular electronic structure whose electronic and dynamic properties are not readily predictable from those of the constituent pigments.)

The diarylethyne-linked multiporphyrin arrays are weakly coupled electronically. The absorption spectra of the arrays are

[†] Los Alamos National Laboratory.
[‡] North Carolina State University.

S1089-5647(97)02304-3 CCC: $15.00 
Published on Web 05/02/1998

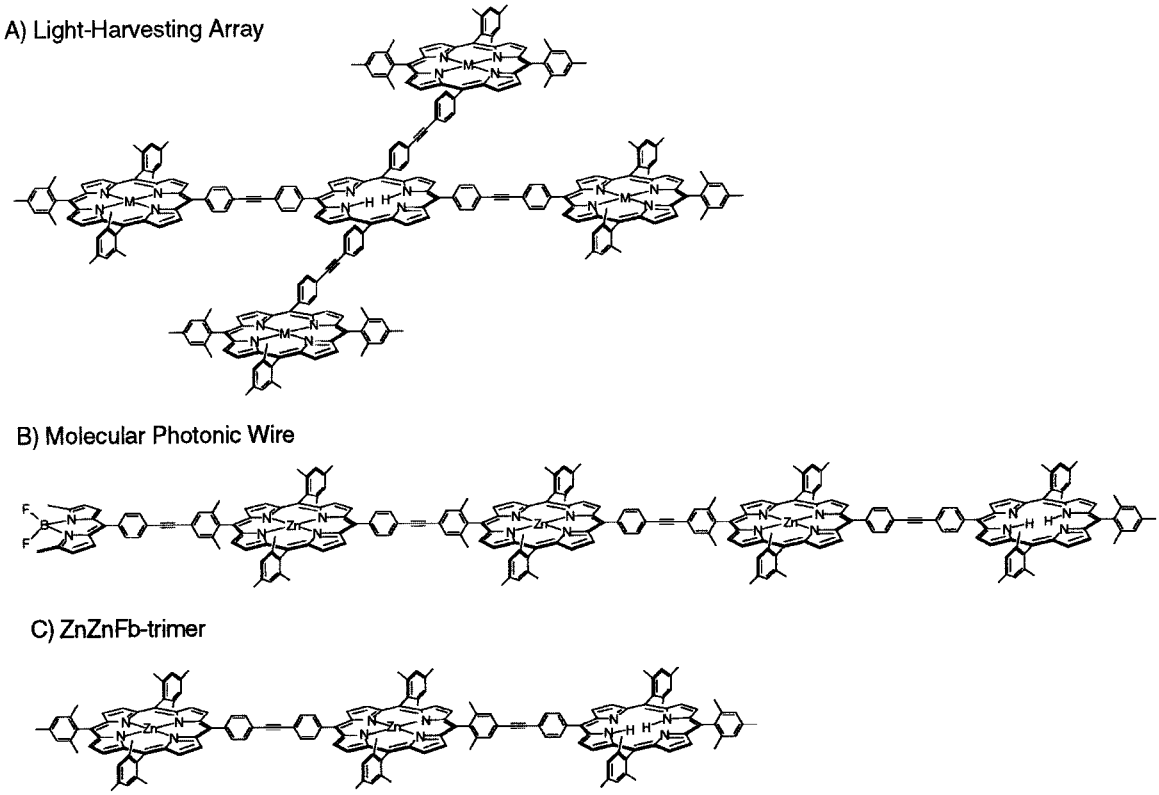


**Figure 1.** Three different diarylethyne-linked arrays: (A) star-shaped pentameric array which behaves as an energy funnel; (B) linear array which constitutes a molecular photonic wire; (C) linear trimer, which serves as a modeling prototype.

essentially a composite of the individual porphyrin spectra, indicating limited excitonic interaction. In diarylethyne-linked arrays that incorporate Zn or Mg tetraarylporphyrins as excited-state energy donors and free base (Fb) tetraarylporphyrins as the terminal energy acceptor, energy transfer occurs with a lifetime of 25−115 ps and quantum efficiency >95%.[35−37] This energy-transfer process occurs in competition with the singlet-state relaxation lifetimes of the donor porphyrins (corresponding to ZnTPP and MgTPP (TPP = tetraphenylporphyrin), 2.4 and 9 ns, respectively).[38] The mechanism of energy transfer primarily involves a through-bond electronic communication process mediated by the diarylethyne linker.[35−37,39,40] The weak electronic coupling and the efficient energy-transfer properties of these arrays makes them well-suited for modeling.

In this paper, we develop analytical methods for simulating the energy-transfer dynamics in weakly coupled multipigment arrays. We use the experimentally determined rates for energy transfer in the diarylethyne-linked porphyrin arrays as a basis for derivation of quantum efficiencies and yields for energy transfer to the terminal acceptor. We then perform a number of simulations to consider various architectures, number of pigments, rate of energy transfer, excited-state lifetime, and energy gradients. Finally we consider various pigments that could be used to realize these designs. While we base the calculations on the experimental behavior of the porphyrinic arrays, this approach is quite general for weakly coupled arrays of light-harvesting chromophores.

## Method

We are interested in the total quantum efficiency (QE) of energy transfer to a terminal acceptor (in this case, a Fb porphyrin) embedded in an array otherwise composed of donor pigments (e.g., Zn porphyrins) that lie energetically "uphill"

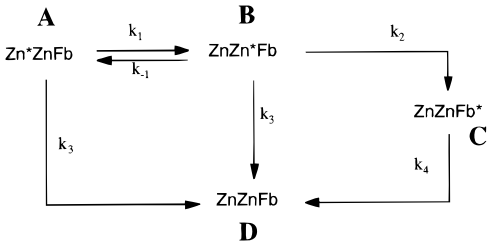


**Figure 2.** Energy-transfer photodynamics in the ZnZnFb trimer with definitions of rate constants.

and among which the excited-state energy migrates in a reversible or irreversible manner. Although the architecture of the arrays can take many forms, with many different structures and incorporation of multiple types of pigments, we begin with simple linear arrays comprised of a single type each of donor and acceptor. Furthermore, we restrict ourselves in all instances to consideration of energy transfer only between nearest neighbor, covalently attached pigments. A trimeric porphyrin array, shown in Figure 1C, serves as a prototype because it embodies many of the critical processes that accompany incoherent energy transfer within any array of weakly coupled pigments. These processes are schematically illustrated in Figure 2 and include energy transfer between the energy donors ($k_1$, $k_{-1}$), energy transfer to the terminal acceptor ($k_2$), and relaxation of the singlet state of the donors ($k_3$). Relaxation of the terminal acceptor ($k_4$) is included for completeness. In general, energy transfer for a porphyrinic array of the form $Zn_{(N-1)}$−Fb can be viewed as a problem of first-order parallel and series reactions with $N + 1$ species. Thus, for the trimer ($N = 3$), it is necessary to consider four configurations, one of which ($D$) is a ground state, or relaxation product.[41] We follow a previously developed formalism for describing general first-order parallel and series reactions.[42]

From Figure 2, it is clear that the pertinent differential equations for the $N = 3$ case are as follows:

$$dA/dt = (-k_1 - k_3)(A) + (k_{-1})(B) \quad (1)$$

$$dB/dt = k_1A + (-k_{-1} - k_2 - k_3)(B) \quad (2)$$

$$dC/dt = k_2B - k_4C \quad (3)$$

$$dD/dt = (k_3)A + (k_3)B + (k_4)C \quad (4)$$

Higher-order problems are formulated in an analogous manner. Note that energy transfer to the acceptor (Fb porphyrin) is assumed here to be an irreversible process ($k_{-2} = 0$), while energy migration among the isoenergetic donors (Zn porphyrins) is modeled with finite forward and reverse rates. Previous experimental data[35,37] support this approach for the specific systems under consideration here.[43−45]

For simplicity, we deviate from the traditional notation[46] and develop the present formalism using matrix notation. Equations 1−4 may be combined into the following equation

$$\mathbf{W}\cdot\mathbf{z} = \frac{d}{dt}\mathbf{z} \quad (5)$$

where

$$\mathbf{z} = \begin{bmatrix} A \\ B \\ C \\ D \end{bmatrix} \quad (6)$$

$$\mathbf{W} = \begin{bmatrix} -k_1 - k_3 & k_{-1} & 0 & 0 \\ k_1 & -k_{-1} - k_2 - k_3 & 0 & 0 \\ 0 & k_2 & -k_4 & 0 \\ k_3 & k_3 & k_4 & 0 \end{bmatrix} \quad (7)$$

We now assume the existence of a real matrix $\mathbf{X}_R$, and its inverse $\mathbf{X}_L$, such that

$$\mathbf{X}_L\cdot\mathbf{W}\cdot\mathbf{X}_R = \lambda \quad (8)$$

where $\lambda$ is diagonal. Since $\mathbf{X}_R$ and $\mathbf{X}_L$ are inverses, we see from (5) that

$$\mathbf{W}\cdot\mathbf{X}_R\cdot\mathbf{X}_L\cdot\mathbf{z} = \frac{d}{dt}\mathbf{z} \quad (9)$$

If we then left-multiply each side by $\mathbf{X}_L$ and use the identity given in (8), we find

$$\lambda\cdot(\mathbf{X}_L\cdot\mathbf{z}) = \frac{d}{dt}(X_L\cdot\mathbf{z}) \quad (10)$$

We define a vector $\mathbf{U}(t) \equiv (\mathbf{X}_L\cdot\mathbf{z})$, whose components, $\mathbf{U}(t)_i$, can be determined from (10) to within the multiplicative constants, $T_i$. The $T_i$ are then determined by imposing initial conditions and solving the equation

$$\mathbf{z} = \mathbf{X}_R\cdot\mathbf{U}(t) \quad (11)$$

Thus, the problem is that of diagonalizing the **W** matrix and using the left and right transformation (eigenvector) matrices to determine the coefficients of the solutions to the differential equations. Several sets of initial conditions are considered below. Unless otherwise mentioned, the initially excited molecular arrays include randomly distributed excitation of the individual Zn porphyrins and no excitation of the Fb porphyrin. (Multiply excited arrays, which could easily be generated depending on the size of the array and photon flux, among other variables, were not considered. The extension of the current method to such a case is problematic in part because the diffusive nature of multiple excited states in these arrays is unknown.) As an alternative to the random excitation of Zn porphyrins, we also modeled the results of excitation at the Zn porphyrin located furthermost from the Fb porphyrin. This notion of remote-donor excitation is of interest for structures such as the "photonic wire", shown in Figure 1B, which includes a boron dipyrromethene dye as the primary energy donor attached to the first Zn porphyrin in a $Zn_3Fb$ linear array.[33]

Following the establishment of initial excitation conditions, we input empirically determined or otherwise relevant values for the required rate constants and then sum over time to determine the percentage of arrays (QE) which reach configuration *C* in Figure 2. The $k_2$ rate is typically chosen to be $(48\ \text{ps})^{-1}$, which is that experimentally determined by examination of the appropriate dimer subunit[35] and is considered to be irreversible.[43] As discussed above, $k_3$ is reasonably assigned to the singlet-state relaxation rate determined elsewhere for the appropriate monomer.[38] Assuming the applicability of the $k_2$ and $k_3$ rates observed for the dimeric arrays, it remains only to assign rates for the energy transfer between the two zinc porphyrins, $k_1$ and $k_{-1}$, to solve for QE in the extended arrays. Because the energy is being transferred between excited states that can reasonably be expected to be isoenergetic, we assume for the moment that $k_1 = k_{-1}$. We have previously used this assumption in numeric modeling of the observed excited-state dynamics of the trimer shown in Figure 1C to derive a value of roughly $(52\ \text{ps})^{-1}$ for $k_1 = k_{-1}$.[35] For convenience, the following rate constant values will be referred to as the "prototypical" values: $k_1 = k_{-1} = (50\ \text{ps})^{-1}$, $k_2 = (48\ \text{ps})^{-1}$, and $k_3 = 2.4$ ns. In general, the results presented herein explore the effects of altering the critical excited-state rate constants, including variations in $k_1$, $k_3$, and $K = k_1/k_{-1}$.

All matrix calculations were performed with MathCad 3.1 or MathCad PLUS 6.0 using typical zero tolerance values of $(10^{15}\ \text{ps})^{-1}$ (this "zero tolerance" represents the maximum value allowed for the off-diagonals of $\lambda$) on a desktop computer (Power Macintosh 7600/132). As a practical matter, satisfactory numerical diagonalization (yielding off-diagonal values very near zero, real eigenvalues, and well-behaved $U(t)_i$ functions) of these matrices sometimes requires replacement of some of the zeroes in the **W** matrix with nonzero values. By keeping these values as small as possible (for example $(10^9-10^{11}\ \text{ps})^{-1}$), errors introduced by these substitutions are kept to a minimum. In fact, the replacement of these elements is the method by which through-space interactions, which will always be nonzero, can be incorporated into these problems. Typical calculations require less than 10 s per array. To check the validity of the calculations, several limiting cases were tested. First, for calculations with $k_3 = 0$, the QE was expected and found to be 1 for all arrays tested. Second, for $k_1 \gg k_2$ the reciprocal of the QE was correctly found to be a linear function of $N - 1$ with slope $k_3/k_2$.[47] Finally, for $k_1 = 0$, the QE was correctly found to be a function of $(N - 1)^{-1}$ with slope $k_2/(k_2 + k_3)$. The MathCad program uses a standard **QL** matrix decomposition for the eigenvalue problems and generates the eigenvectors via inverse iteration.[48]

The QE measures the fraction of those arrays where an absorbed photon results in an exciton reaching the trap. An equally important measure of performance concerns the light-gathering efficiency of different types of arrays. A ZnFb dimer

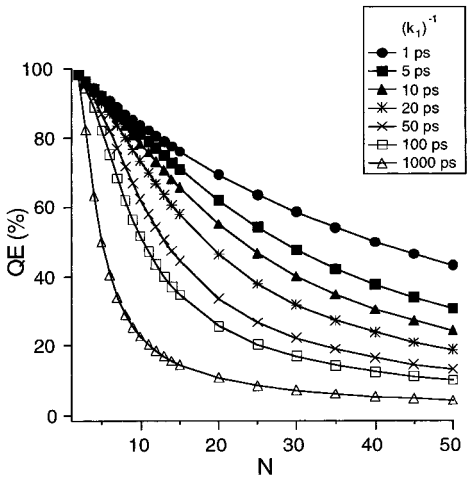


**Figure 3.** Quantum efficiency of energy migration to a terminal trap in linear arrays of $N$ pigments for various $k_1$ values. All $(N - 1)$ donor pigments are assumed to absorb equally. ($k_{-1} = k_1$; $k_2 = (48\ \text{ps})^{-1}$; $k_3 = (2.4\ \text{ns})^{-1}$.)

and the corresponding star-shaped $Zn_4Fb$ pentamer have identical QE values, but the latter is a more efficient light-gathering device. The greater light-harvesting effectiveness of the pentamer stems from its larger antenna. We assess the antenna effect (AE) by the relation shown below,

$$\text{AE} = (N - 1)(\text{QE}_{N-\text{mer}}) \tag{12}$$

where $N - 1$ is the number of donor pigments in the array and QE is as defined above. In effect the AE takes into account the increased cross-section that accompanies expansion of the donor pigment pool. This equation assumes all donor pigments are identical, thereby avoiding the necessity to include individual extinction coefficients. Further, this relation is applicable only in the linear absorption limit, i.e., under the approximation that additional pigments boost the cross-section in an additive manner. After having determined the QE for a variety of arrays, we will also evaluate the antenna effect of several arrays and address how arrays can be designed for increased light-harvesting capacity.

## Results and Discussion

In this section, we first consider the QE of energy migration to a terminal porphyrin from isoenergetic pigments in linear arrays. Then we explore the effects of altering the rates of the energy transfer between the pigments ($k_1$, $k_{-1}$) and of the competitive relaxation processes ($k_3$). Variation of $k_2$ is not explored because this parameter is typically unimportant for QE in extended arrays, as long as $k_3/k_2 \ll 1$. We also examine the results of assembling pigments in clustered or ring architectures. Next, we turn to the effects of incorporating energy gradients in these architectures. We conclude with a discussion of the various components for realizing these designs, emphasizing the tunability of electronic structure provided by porphyrinic pigments.

**Linear Arrays of Isoenergetic Pigments.** We have calculated energy-transfer efficiencies for a variety of linear "*N*-mers". In such structures, all donor chromophores absorb equally and a trap is positioned at one end of the linear array. Figure 3 shows plots of QE versus $N$ as obtained for several different energy-transfer rate constants ($k_1$), with $k_2$ and $k_3$ fixed at their prototypical values and $k_{-1} = k_1$. Of course, QE values only exist for integral values of $N$. The lines between data points in this and in subsequent plots merely serve as a guide to the eye.

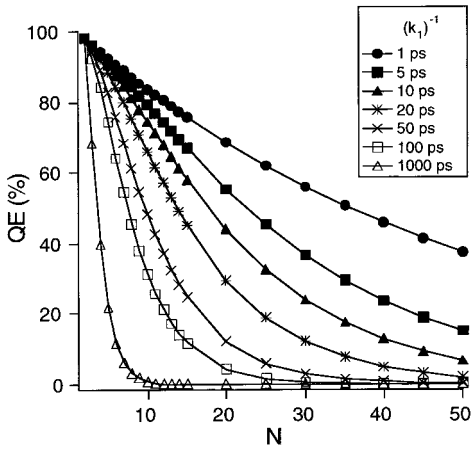


**Figure 4.** Quantum efficiency of energy migration to a terminal trap in linear arrays of $N$ pigments for various $k_1$ values. Excitation occurs only at the terminal donor pigment. ($k_{-1} = k_1$, $k_2 = (48\ \text{ps})^{-1}$; $k_3 = (2.4\ \text{ns})^{-1}$.)

The trace representing QE for a linear array with $k_1 = (50\ \text{ps})^{-1}$, which coincides with the approximate transfer rate determined for the isoenergetic Zn porphyrins in the ZnZnFb trimer,[35] is of interest. In this case the calculations indicate that the QE falls to 50% at a length of about 14 porphyrin units. The error limits established previously for $k_1$, $\pm(19\ \text{ps})^{-1}$,[35] bracket the predicted 50% QE length as $13 \leq N \leq 16$.

This simulation clearly demonstrates the strong dependence of QE upon changes in $k_1$. For example, the QE for trapping the excitation is only 35% for a linear array of 20 porphyrins with a transfer rate $k_1$ of $(50\ \text{ps})^{-1}$ among isoenergetic porphyrins. However, a transfer rate of $(1\ \text{ps})^{-1}$, which is a reasonable upper limit for weakly coupled chromophores, results in 70% efficiency for such an array, and 43% QE for a linear array of 50 porphyrins. Thus, increasing the rate of transfer improves the quantum efficiency, but a 50-fold increase in rate is insufficient in providing high efficiency (>90%) for linear arrays of more than a handful of isoenergetic porphyrins.

How far can energy migrate in a linear array without significant loss? The previous simulations addressed this issue in an indirect manner, as excitation occurs equally at all donor chromophores. However, structures such as the molecular photonic wire (Figure 1B),[33] where excitation can be introduced predominantly at a terminal boron dipyrromethene dye attached to the first Zn porphyrin in a linear array, have motivated this question. To simulate the behavior of arrays wherein excitation and trapping occur at opposite ends, the initial conditions have been chosen so that excitation occurs only at the donor furthermost from the acceptor. In this case, a linear array of 20 porphyrins with excited-state dynamics determined by the prototypical rate constants exhibits a QE of only 13%. Plots of QE as a function of $k_1$ and array length under such initial excitation conditions are shown in Figure 4.

**Effects of Excited-State Lifetime.** Energy migration must compete with the intrinsic lifetime of the excited state. We recently compared the photodynamics of MgFb and ZnFb porphyrin dimers.[37] The rate of energy transfer is essentially identical in the two systems; however, the intrinsic lifetime of MgTPP is 9 ns, while that of ZnTPP is 2.4 ns,[38] resulting in greater QE in the MgFb dimers. Accordingly, we examined the predicted effects of changes in the intrinsic singlet-excited-state lifetime on energy-migration efficiencies in linear arrays. The results for linear arrays with the prototypical values of $k_1$ and $k_3$ are shown in Figure 5. A comparison of QE for linear arrays with competitive deactivation rates of 1, 2.4, 5, 9, and

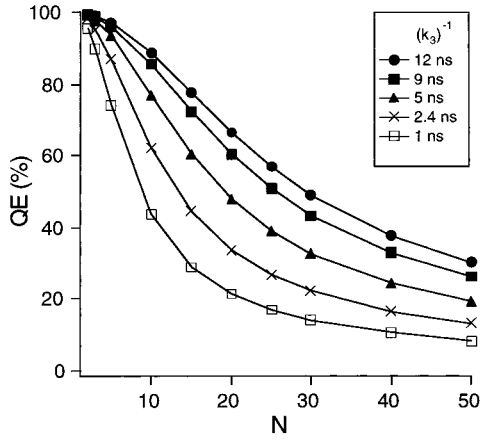


**Figure 5.** Quantum efficiency of energy migration to a terminal trap in linear arrays of $N$ pigments for various $k_3$ values. All donor pigments are assumed to absorb equally. ($k_1 = k_{-1} = (50\ \text{ps})^{-1}$; $k_2 = (48\ \text{ps})^{-1}$.)

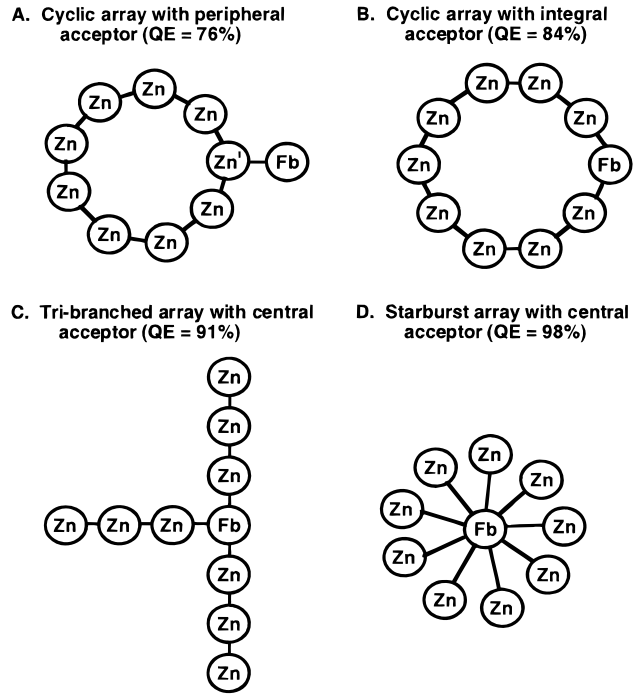


**Figure 6.** Effect of architecture on quantum efficiency of energy migration to a lone trap in cyclic (A, B) and branched (C, D) arrays containing nine donor pigments. All donor pigments are assumed to absorb equally. ($k_1 = k_{-1} = (50\ \text{ps})^{-1}$, $k_2 = (48\ \text{ps})^{-1}$, $k_3 = (2.4\ \text{ns})^{-1}$.)

12 ns reveals a significant enhancement with increased excited-singlet-state lifetime. As an example, the calculations predict that for $Zn_9Fb$ and $Mg_9Fb$ linear arrays the QEs are 62 and 85%, respectively, while for linear 20-mers the predicted QEs are 34 and 60%, respectively.

**Cluster Arrays.** The previous arrays consisted of linear 1-D arrangements of porphyrins. We now consider a variety of cyclic and branched arrays (Figure 6). The QE for each of these two-dimensional arrangements of porphyrins is determined for geometries with nine Zn porphyrins and one Fb porphyrin, again using the prototypical rate constants. For comparison, a linear array of nine Zn porphyrins and one terminal Fb porphyrin exhibits a QE of 63%. The first example is a cyclic array of Zn porphyrins with a Fb porphyrin acceptor attached to a single Zn porphyrin, indicated by Zn′ (Figure 6A). Compared with the linear analogue, this structure decreases the number of energy-transfer steps between the Fb porphyrin and the most remote Zn porphyrin and provides multiple paths for the energy transfer to Zn′, whereupon energy transfer to the Fb can occur. This has the effect of increasing the predicted QE to 76%, slightly greater than that of the corresponding linear array. The second example is a cyclic array of Zn porphyrins with an integral Fb acceptor (Figure 6B). In this case, the QE is increased to 84%. The additional efficiency seen for this array results from the presence of two direct paths to the Fb acceptor, in contrast to the single path in the array in Figure 6A. Furthermore, an exciton reaching Zn′ in Figure 6A has two exit paths in addition to transfer to the Fb acceptor, while an exciton reaching a Zn porphyrin adjacent to the Fb acceptor in Figure 6B has only one such alternative. The third example consists of independent linear branches attached to a core Fb porphyrin. This architecture yields a QE identical to that of the linear tetramer (91%). Essentially, this array is comprised of three such linear tetramers sharing a common acceptor. The fourth example consists of a star-shaped array where every Zn porphyrin is directly attached to the Fb porphyrin. In effect this structure is analogous to nine ZnFb dimers, where the Fb porphyrin is common to each of the donors. The QE of this array is 98%, which is identical to that of a ZnFb dimer.

The predicted efficiencies of the arrays in Figure 6A−D illustrate a concept that is universally applicable in the design of energy-transfer arrays. Because the competition with excited-state relaxation is so critical for achieving high yields, significant increases in QE can be obtained in arrays of a given composition by selecting an architecture that minimizes the number of nonproductive energy-transfer steps. This effect is clearly revealed by the comparison of the branched 10-mer arrays in Figure 6 with their linear counterpart. Of course, practical issues such as steric crowding and increased through-space interactions will limit the realization of efficient cluster arrays.

**Cascade Arrays.** In the previous simulations, we have assumed that energy travels along the array backbone in a random walk fashion ($k_1 = k_{-1}$). While this model is consistent with data obtained from systems examined to date, the stipulation that $k_1$ equals $k_{-1}$ is justified only for transfers between isoenergetic pigments. Multiple types of donors within an array can be used to increase the ratio of the forward to reverse rates, making $K = k_1/k_{-1} > 1$. Such an arrangement would result in directed energy transfer and enhanced QE. As an illustration, we have investigated the effect of decreasing the reverse transfer rate for each donor−donor transfer ($K > 1$) while retaining a forward transfer rate ($k_1$) of $(50\ \text{ps})^{-1}$. With the exception of $k_{-1}$, we use the prototypical rate constants. Note that the resulting QE plots, shown in Figure 7, reveal an initially rapid increase in QE for a given linear array as $K$ increases above 1. As an example, inspection of the results for $K = 2$ reveals that this QE curve closely resembles that given by arrays with $K = 1$ but with $k_1 = k_{-1} = (1\ \text{ps})^{-1}$ (see Figure 3). Thus, for $k_1 = (50\ \text{ps})^{-1}$, a 2-fold decrease in the reverse rate yields about the same improvement in QE as a 50-fold increase in the energy-transfer rates within a linear array in which the exciton migrates in a random walk. Although such an array has not yet been synthesized, this calculation demonstrates that modest retardation of reverse transfers can yield QE enhancements similar to those obtained with dramatic increases in both forward and reverse rates of energy transfer among isoenergetic pigments.

For the data in Figure 7, we find that the influence of $K$ on QE diminishes quickly above $K = 5$. The QE values obtained for $K = \infty$ are increased relative to those for $K = 10$ by roughly the same amount that the values for $K = 10$ are greater than those for $K = 5$. (These last two traces are truncated due to convergence problems with the program. The data for $K = \infty$

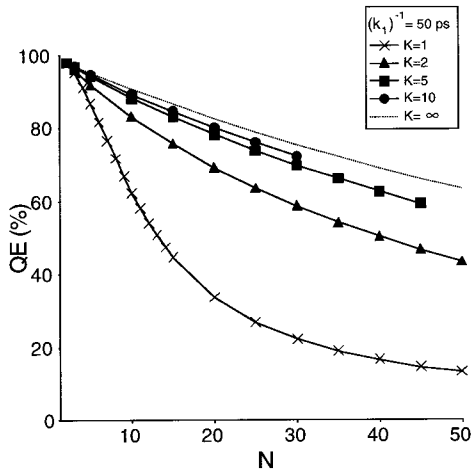


**Figure 7.** Quantum efficiency of energy migration to a terminal trap in linear arrays of $N$ pigments for various $K$ ($=k_1/k_{-1}$) values. All donor pigments are assumed to absorb equally. ($k_1 = (50\text{ ps})^{-1}$; $k_2 = (48\text{ ps})^{-1}$; $k_3 = (2.4\text{ ns})^{-1}$.) Several data points are missing from the $K = 5$ and $K = 10$ plots due to the failure of the MathCad algorithm to converge on a real solution for these $K$ values. The $K = \infty$ line is derived by an analytical expression.

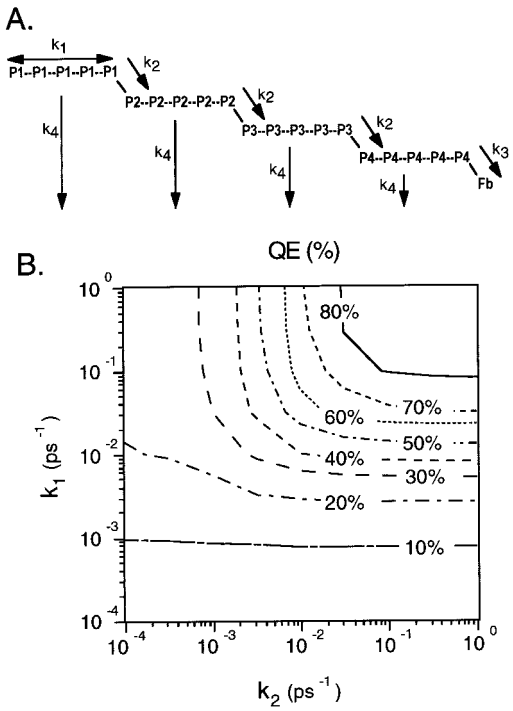


**Figure 8.** (A) Prototypical 21-mer cascade array of pigments ($P_N$) with definitions of rate constants. (B) Contour plot of quantum efficiency of energy migration to a terminal trap in the prototypical 21-mer cascade array as a function of $k_1$ and $k_2$. All donor chromophores are assumed to absorb equally. ($k_3 = (48\text{ ps})^{-1}$; $k_4 = (2.4\text{ ns})^{-1}$.)

are obtained by derivation of an analytical expression.) Thus, only modest forward and reverse rate differentials are needed to induce a high degree of vectorial character in the energy-transfer process.

An energy cascade also can be incorporated through the use of a cataract architecture comprised of pools of isoenergetic chromophores, as outlined in Figure 8A. This linear 21-mer uses four different donor porphyrins ($P_1-P_4$). Porphyrins of the same type are isoenergetic and are assumed to behave so that $K = k_1/k_{-1} = 1$. Conversely, transfer between unlike donors is accompanied by an energetic downstep and occurs irreversibly with rate $k_2$. Transfer to the terminal acceptor is here characterized by $k_3$ and is assumed to be equivalent to the irreversible Zn−Fb transfer ($k_3 = (48\text{ ps})^{-1}$). A single rate constant, $k_4 = (2.4\text{ ns})^{-1}$, characterizes the relaxation of all of the donors. This problem has a large number of parameters and in the general case would be quite complex. For example, the general case would have four different $k_1$'s and $k_4$'s (one each for every type of donor), three different $k_2$'s, as well as distinct reverse rates. To demonstrate the performance potential of this cascade architecture, we restrict ourselves to the simple case outlined above.

The contour plot in Figure 8B shows the QE for this system plotted as a function of transfer rates $k_1$ and $k_2$. For the prototypical values of $(50\text{ ps})^{-1}$ and $(48\text{ ps})^{-1}$, respectively, the QE is ∼55% (cf. the linear 20-mer result of ∼35%). The plot provides details regarding the comparative effects of varying $k_1$ and $k_2$. Of course, the highest QE is observed when both $k_1$ and $k_2$ are fast (upper right corner). Within the region defined by variation of both rates between $(10\text{ ps})^{-1}$ and $(100\text{ ps})^{-1}$, the contours are much more dense along the $k_1$ axis than the $k_2$ axis, demonstrating for this regime that efficient reversible energy transfer among isoenergetic pigments ($k_1$) outweighs the importance of imposing a rapid irreversible rate between individual pools ($k_2$). Conversely, for very rapid $k_1$ rates ($>(10\text{ ps})^{-1}$), the contours are much more dense along the $k_2$ axis between $(10\text{ ps})^{-1}$ and $(100\text{ ps})^{-1}$ so that, in this regime, increases in $k_2$ are much more influential upon QE than are increases in $k_1$. These results demonstrate that the design of such cascade arrays must consider the fact that either of the rates of energy transfer (within or between pigment pools) can be predominant in determining the QE.

**Antenna Effect.** As the donor pool within an array is expanded, the QE will be diminished if the number of nonproductive energy-transfer steps is increased. The tradeoff between increasing the donor pool and any reduction in QE is measured by the antenna effect (AE), defined in Method. The AE is ideally suited for assessing the light-harvesting performance of arrays. For example, the ZnFb dimer and the corresponding star-shaped $Zn_4Fb$ pentamer each have QE = 0.98, but the AE of the former is 0.98 while that of the latter is 3.92. An additional comparison is provided by the linear arrays. A linear 10-mer has QE = 63% and AE = 5.67, while a linear 20-mer has QE = 35% but AE = 6.65. The longer array has diminished quantum efficiency but is a marginally better light-gathering device. This slight increase in performance has occurred at the expense of a doubling of the donor pool. The AE for linear arrays as a function of $k_1$ is displayed in Figure 9. As $k_1$ increases, progressively larger donor pools give increased performance. Thus, for $k_1 = (10\text{ ps})^{-1}$ the light-harvesting performance levels off at about 30 donor pigments (i.e., additional donor pigments give no increase in AE), while for $k_1 = (1\text{ ps})^{-1}$ the performance is still increasing with 50 donor pigments.

The AE provides a tool for assessing other array design strategies. In terms of energy capture at the acceptor, the most productive modification of a given array architecture will be that which most increases the AE. As an example, consider the addition of three donors to the array in Figure 6C, which has AE = 8.19 and QE =91%. Adding a single Zn porphyrin to the end of each existing branch decreases QE to 87% (equaling that of a linear pentamer), while the AE increases to 10.44. An alternative option is to attach a fourth linear array of three Zn porphyrins directly to the Fb porphyrin, forming a symmetrical cross-shaped array. Attaching a fourth linear array causes no change in QE (since the four linear $Zn_3$ trimers are

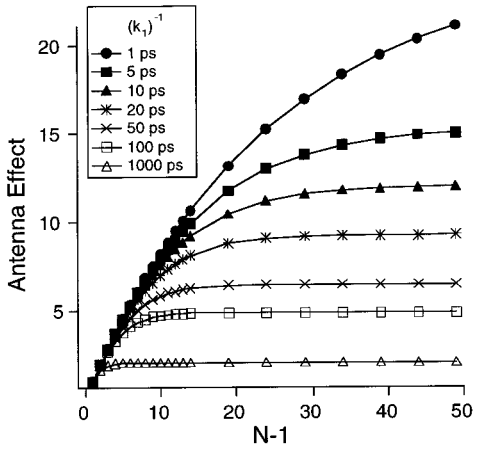


**Figure 9.** Antenna effect (performance factor for light harvesting at a terminal trap) in linear oligomeric arrays of $N$ pigments for various $k_1$ values. All $(N - 1)$ donor pigments are assumed to absorb equally. ($k_{-1} = k_1$, $k_2 = (48\ \text{ps})^{-1}$; $k_3 = (2.4\ \text{ns})^{-1}$.)

independent), but AE increases to 10.92. These calculations show the most efficient way to increase the light-gathering capacity by increasing the size of the donor pool. Creating a new independent path for additional donors to funnel energy directly to the acceptor is a more efficient design than increasing the size of existing donor pools. The addition of new pathways does not increase the possibility of nonproductive transfers in the existing donor pool, as occurs when the existing pools are merely increased in size. This design feature reaches its zenith by the architecture shown in Figure 6D. Here, the QE is equal to that of a dimer (98%), and the AE exhibits a linear dependence on the number of attached donors.

**Molecular Design Considerations.** The versatility of porphyrinic pigments provides a host of avenues for manipulating the interpigment communication rates and transfer efficiencies ($k_1$, $k_{-1}$, and $k_3$). We have already seen that $k_3$ can be changed by selection of the coordinated metal. The $k_1$ rate can be modified by a variety of methods, including alterations in the length and electronic structure of the linker, orbital ordering,[36] and the site of connectivity of the linker to the chromophores. However, these manipulations will alter both $k_1$ and $k_{-1}$. Tuning the excited-state energy levels of sequential donor macrocycles within an array provides a means of achieving directed energy transfer ($K > 1$). A collection of diverse porphyrinic pigments with long-wavelength maxima ranging from 572 to 780 nm is shown in Table 1.[49−67] Further tuning of excited-state energy levels can be achieved with other expanded porphyrins,[68] isomeric porphyrins,[69] phthalocyanines bearing various numbers of alkoxy groups,[70] and heteroatom-substituted hydroporphyrins. Specific examples of graded arrays include the following: (1) A linear composition of porphyrin, chlorin, and bacteriochlorin pigments, where the longest wavelength absorption band moves from 646 nm, 655 nm, to 740 nm, respectively. (2) A sequential array of heteroatom-substituted porphyrins, such as tetraphenylporphyrin (646 nm), $N_3O$−porphyrin (654 nm), $N_3S$−porphyrin (675 nm), NONS−porphyrin (691 nm), and NSNS−porphyrin (699 nm), would provide a fine gradation of energy levels. These cascades should direct the excited-state down a progressive energy funnel.

To predict the QE for such hypothetical arrays by the present approach would require experimental or theoretical determination of the rates associated with each pairwise interaction. In addition to concerns about energy levels, deleterious photodynamic processes must be avoided in order to achieve efficient energy migration. For example, the excited-state lifetime of each pigment must be sufficiently long so as not to cause decay of the exciton. In the heteroatom-substituted porphyrins, an $N_3S$−porphyrin has fluorescence quantum yield $\Phi_f = 0.0168$ and singlet excited-state lifetime $\tau = 1.36$ ns,[71] an NSNS−porphyrin has $\Phi_f = 0.0076$[71] and $\tau = 1.30$ ns,[72] but the NSNSe− or NSeNSe−porphyrin has $\Phi_f < 10^{-5}$,[72] suggesting a very short-lived excited state. In addition, the prospect of electron-transfer quenching interactions must be considered upon signficant alteration of energy levels of adjacent pigments. These factors must be assessed experimentally prior to simulation of energy-transfer rates and efficiencies in multipigment arrays.

**TABLE 1: Spectroscopic Properties of Selected Porphyrinic Pigments**

| pigment | $\lambda_{abs}$[a] | $E$ (eV) |
|---|---|---|
| Zn-octaethylporphyrin | 572[49] | 2.17 |
| Zn-tetraphenylporphyrin | 586[50] | 2.12 |
| $Et_2Me_6$corrole | 593[51] | 2.09 |
| Mg-tetraphenylporphyrin | 604[52] | 2.05 |
| tetraazaporphyrin | 617[53] | 2.01 |
| Zn-tetraphenylchlorin | 622[54] | 1.99 |
| octaethylporphyrin | 622[55] | 1.99 |
| Zn-tetrabenzporphyrin | 624[56] | 1.99 |
| *trans*-octaethylchlorin | 646.5[57] | 1.92 |
| tetraphenylporphyrin | 647[58] | 1.92 |
| *cis*-octaethylchlorin | 651[57] | 1.90 |
| tetraphenylchlorin | 652[59] | 1.90 |
| $N_3O$−porphyrin[b] | 664[60] | 1.87 |
| Zn-phthalocyanine | 672[61] | 1.84 |
| Mg-phthalocyanine | 674.5[61] | 1.84 |
| $N_3S$-porphyrin[c] | 680[62] | 1.82 |
| NSNO-porphyrin[d] | 691[63] | 1.79 |
| $R_{10}$-pentaphyrin | 695[64] | 1.78 |
| phthalocyanine | 698[61] | 1.78 |
| NSNS-porphyrin[e] | 699[65] | 1.77 |
| NONO-porphyrin[f] | 704[60] | 1.76 |
| *trans*-tetraphenylbacteriochlorin | 742[59] | 1.67 |
| Zn-*trans*-tetraphenylbacteriochlorin | 745[66] | 1.66 |
| naphthalocyanine | 780[67] | 1.59 |

[a] $\lambda_{abs}$ is the longest wavelength absorption maximum. [b] 5-Phenyl-10,15-bis(*p*-tolyl)-21-oxaporphyrin. [c] *meso*-Tetrakis(*p*-tolyl)-21-thiaporphyrin. [s] *meso*-Tetraphenyl-21-oxa-23-thiaporphyrin. [e] *meso*-Tetraphenyl-21,23-dithiaporphyrin. [f] *meso*-Tetraphenyl-21,23-dioxaporphyrin.

## Conclusions

Light harvesting in molecular arrays depends on the efficient absorption of light and transfer of energy to a terminal acceptor with minimal loss of energy during the energy-migration process. The present modeling approach permits facile calculation of the quantum efficiency of the energy-migration process as well as the antenna effect in a wide assortment of arrays. The ability to evaluate the expected performance of each architecture under consideration permits synthetic efforts to be directed toward effective light-harvesting structures.

**Acknowledgment.** This work was supported at Los Alamos National Laboratory by a Laboratory Directed Research and Development grant and at North Carolina State University by a grant from the Division of Chemical Sciences, Office of Basic Energy Sciences, Office of Energy Research, U.S. Department of Energy.

## References and Notes

(1) Boxer, S. G. *Biochim. Biophys. Acta* **1983**, *726*, 265.
(2) Gust, D.; Moore, T. A. *Science* **1989**, *244*, 35.
(3) Borovkov, V. V.; Evstigneeva, R. P.; Strekova, L. N.; Filippovich, E. I. *Russ. Chem. Rev.* **1989**, *58*, 602.
(4) Gust, D.; Moore, T. A. *Top. Curr. Chem.* **1991**, *159*, 103.

(5) Wasielewski, M. R. In *Chlorophylls*; Scheer, H., Ed.; CRC Press: Boca Raton, FL, 1991; p 269.

(6) Wasielewski, M. R. *Chem. Rev.* **1992**, *92*, 435.

(7) Gust, D.; Moore, T. A.; Moore, A. L. *Acc. Chem. Res.* **1993**, *26*, 198.

(8) Gribkova, S. E.; Evstigneeva, R. P.; Lizgina, V. N. *Russ. Chem. Rev.* **1993**, *62*, 963.

(9) Kurreck, H.; Huber, M. *Angew. Chem., Int. Ed. Engl.* **1995**, *34*, 849.

(10) Osuka, A.; Tanabe, N.; Zhang, R. P.; Maruyama, K. *Chem. Lett.* **1993**, *9*, 1505.

(11) Vidal-Ferran, A.; Clyde-Watson, Z.; Bampos, N.; Sanders, J. K. M. *J. Org. Chem.* **1997**, *62*, 240.

(12) Anderson, S.; Anderson, H. L.; Sanders J. K. M. *J. Chem. Soc., Perkin Trans. 1* **1995** 2255.

(13) Fenyo, D.; Chait, B. T.; Johnson, B. T.; Lindsey, J. S. *J. Porph. Phthalocy.* **1997**, *1*, 93.

(14) Wagner, R. W.; Johnson, T. E.; Lindsey, J. S. *J. Am. Chem. Soc.* **1996**, *118*, 11166.

(15) Prathapan, S.; Johnson, T. E.; Lindsey, J. S. *J. Am. Chem. Soc.* **1993**, *115*, 7519.

(16) Milgrom, L. *J. Chem. Soc., Perkin Trans. 1* **1983**, 2535.

(17) Wennerstrom, O.; Ericsson, H.; Raston, I.; Svensson, S.; Pimlott, W. *Tetrahedron Lett.* **1989**, *30*, 1129.

(18) Nagata, T.; Osuka, A.; Maruyama, K. *J. Am. Chem. Soc.* **1990**, *112*, 3054.

(19) Aota, H.; Itai, Y.; Matsumoto, A.; Kamachi, M. *Chem. Lett.* **1994**, 2043.

(20) Segawa, H.; Kunimoto, K.; Susumu, K.; Taniguchi, M.; Shimidzu, T. *J. Am. Chem. Soc.* **1994**, *116*, 11193.

(21) Ichihara, K.; Naruta, Y. *Chem. Lett.* **1995**, 631.

(22) Osuka, A.; Tanabe, N.; Nakajima, S.; Maruyama, K. *J. Chem. Soc., Perkin Trans. 2* **1996**, 199.

(23) Officer, D. L.; Burrell, A. K.; Reid, D. C. W. *J. Chem. Soc., Chem. Commun.* **1996**, 1657.

(24) Xu, Z.; Moore, J. S. *Acta Polym.* **1994**, *45*, 83.

(25) Drain, C. M.; Lehn, J. M. *J. Chem. Soc., Chem. Commun.* **1994**, 2313.

(26) Chi, X.; Guerin, A. J.; Haycock, R. A.; Hunter, C. A. Sarson, L. D. *J. Chem. Soc., Chem. Commun.* **1995**, 2567.

(27) (a) Miyaji, H.; Kobuke, Y.; Kondo, J. *Chem. Lett.* **1996**, 497. (b) Kobuke, Y.; Miyaji, H. *Bull. Chem. Soc. Jpn.* **1996**, *69*, 3563.

(28) Tamiaki, H.; Amakawa, M.; Shimono, Y.; Tanikaga, R.; Holzwarth, A. R.; Schaffner, K. *Photochem. Photobiol.* **1996**, *63*, 92.

(29) Alessio, E.; Macchi, M.; Heath, S.; Marzilli, L. G. *Chem. Commun.* **1996**, 1411.

(30) Kariya, N.; Imamura, T.; Sasaki, Y. *Inorg. Chem.* **1997**, *36*, 833.

(31) Denti, G.; Serroni, S.; Campagna, S.; Juris, A.; Balzani, V. *Mol. Cryst. Liq. Cryst.* **1993**, *234*, 79.

(32) Bothner-By, A. A.; Dadok, J.; Johnson, T. E.; Lindsey, J. S. *J. Phys. Chem.* **1996**, *100*, 17551.

(33) Wagner, R. W.; Lindsey, J. S. *J. Am. Chem. Soc.* **1994**, *116*, 9759.

(34) Wagner, R. W.; Lindsey, J. S.; Seth, J.; Palaniappan, V.; Bocian, D. F. *J. Am. Chem. Soc.* **1996**, *118*, 3996.

(35) Hsiao, J.-S.; Krueger, B. P.; Wagner, R. W.; Johnson, T. E.; Delaney, J. K.; Mauzerall, D. C.; Fleming, G. R.; Bocian, D. F.; Lindsey, J. S.; Donohoe, R. J. *J. Am. Chem. Soc.* **1996**, *118*, 11181.

(36) Strachan, J. P.; Gentemann, S.; Seth, J.; Kalsbeck, W. A.; Lindsey, J. S.; Holten, D.; Bocian, D. F. *J. Am. Chem. Soc.* **1997**, *119*, 11191.

(37) Li, F.; Gentemann, S.; Kalsbeck, W. A.; Seth, J.; Lindsey, J. S.; Holten, D.; Bocian, D. F. *J. Mater. Chem.* **1997**, *7*, 1245.

(38) (a) Rodriguez, J.; Kirmaier, C.; Holten, D. *J. Am. Chem. Soc.* **1989**, *111*, 6500. (b) Gradyushko, A. T.; Tsvirko, M. P. *Opt. Spectrosc.* **1971**, *31*, 291. (c) Harriman, A. *J. Chem. Soc., Faraday Trans.* **1981**, *2*, 1281. (d) Politis, T. G.; Drickamer, H. G. *J. Chem. Phys.* **1982**, *76*, 285. (e) Ohno, O.; Kaizu, Y.; Kobayashi, H. *J. Chem. Phys.* **1985**, *82*, 1779.

(39) Seth, J.; Palaniappan, V.; Johnson, T. E.; Prathapan, S.; Lindsey, J. S.; Bocian, D. F. *J. Am. Chem. Soc.* **1994**, *116*, 10578.

(40) Seth, J.; Palaniappan, V.; Wagner, R. W.; Johnson, T. E.; Lindsey, J. S.; Bocian, D. F. *J. Am. Chem. Soc.* **1996**, *118*, 11194.

(41) We do not distinguish between various possible relaxation products, e.g. between excited triplet and ground states; however, we note that energy transfer between triplet states is a possibility[42] and that the primary relaxation pathway of singlet-excited ZnTPP is known to be relaxation to the triplet excited state.[38a] Our assumption that the energy transfer is limited to singlet-state dynamic processes indicates that the calculated quantum efficiencies represent a lower bound.

(42) Lamola, A. A. In *Energy Transfer and Organic Photochemistry*, Leermakers, P. A., Weissberger, A., Eds.; Interscience: New York, 1969; p 25.

(43) Previous experimental results[37] for multiply branched arrays (pentamers comprised of a central Fb porphyrin directly attached to four independent Mg or Zn porphyrins) demonstrate that the QE of energy transfer actually exceeds that of the analogous dimer. This is likely due to comparative stabilization of the Fb porphyrin in the pentamer, where none of the aryl substituents include sterically hindering groups next to the macrocycle. More importantly, the pentamer results suggest that energy transfer from Zn or Mg porphyrins to the Fb porphyrin in the diarylethyne-linked arrays is irreversible. Otherwise, slower observed energy-transfer rates might be expected for the pentamers due to the 4-fold increase in the number of potential energy acceptors once the transfer to the cental Fb porphyrin has taken place. The apparent lack of reverse energy transfer for these arrays is in contrast to the theoretical[44] and experimental[45] results for coupled light-harvesting and reaction center proteins, where energy transfer from the reaction center back to the light-harvesting protein is known. The ability to include nonzero $k_{-2}$ rates would require only minor modifications of the program.

(44) Pearlstein, R. M. *Photochem. Photobiol.* **1982**, *35*, 835.

(45) Owens, T. G.; Webb, S. P.; Mets, L.; Alberte, R. S.; Fleming, G. R. *Proc. Natl. Acad. Sci. U.S.A.* **1987**, *84*, 1532.

(46) (a) Moore, J. W.; Pearson, R. G. *Kinetics and Mechanism*, 3rd ed.; John Wiley & Sons: New York, 1981; pp 296−300, and references cited therein. (b) Zwolinski, B. J.; Eyring, H. *J. Am. Chem. Soc.* **1947**, *69*, 2702. (c) Matsen, F. A.; Franklin, J. L. *J. Am. Chem. Soc.* **1950**, *72*, 3337.

(47) This result is readily derived by recognizing that, under such conditions, the rapid exchange of energy among the donors yields what may be considered to be a single "super" donor, transferring energy to the acceptor (rate $k_2$) in competition with $N - 1$ relaxation paths (rate $k_3$). Then, the QE is equal to the ratio of the rate of transfer from the super donor to the acceptor divided by the sum of all transfer rates, which is $k_2 + (N - 1)k_3$.

(48) For an explanation of these methods, see: (a) Wilkinson, J. H. In *Linear Algebra*; Bauer, F. L., Ed.; Springer-Verlag: New York, 1971; pp 191−201. (b) Press: W. H.; Flannery, B. P.; Teukolsky, S. A.; Vetterling, W. T. *Numerical Recipes*; Cambridge University Press: Cambridge, U.K., 1986; Chapter 11.

(49) Ballard, S. G.; Mauzerall, D. C. *J. Chem. Phys.* **1980**, *72*, 933.

(50) Quimby, D. J.; Longo, F. R. *J. Am. Chem. Soc.* **1975**, *97*, 5111.

(51) Johnson, A. W.; Kay, I. T. *J. Chem. Soc.* **1965**, 1620.

(52) Lindsey, J. S.; Woodford, J. N. *Inorg. Chem.* **1995**, *34*, 1063.

(53) Stuzhin, P. A.; Khelevina, O. G. *Coord. Chem. Rev.* **1996**, *147*, 41.

(54) Miller, J. R.; Dorough, G. D. *J. Am. Chem. Soc.* **1952,** *74*, 3977.

(55) Eisner, U.; Lichtarowicz, A.; Linstead, R. P. *J. Chem. Soc.* **1957**, 733.

(56) Bajema, L.; Gouterman, M.; Rose, C. B. *J. Mol. Spectrosc.* **1971**, *39*, 421.

(57) Inhoffen, H. H.; Buchler, J. W.; Thomas, R. *Tetrahedron Lett.* **1969**, *14*, 1145.

(58) Kim, J. B.; Leonard, J. J.; Longo, F. R. *J. Am. Chem. Soc.* **1972**, *94*, 3986.

(59) Whitlock, H. W., Jr.; Hanauer, R.; Oester, M. Y.; Bower, B. K. *J. Am. Chem. Soc.* **1969**, *91*, 7485.

(60) Chmielewski, P. J.; Latos-Grazynski, L.; Olmstead, M. M.; Balch, A. L. *Chem. Eur. J.* **1997**, *3*, 268.

(61) Whalley, M. *J. Chem. Soc.* **1961**, 866.

(62) Latos-Grazynski, L.; Lisowski, J.; Olmstead, M. M.; Balch, A. L. *J. Am. Chem. Soc.* **1987**, *109*, 4428.

(63) Heo, P. Y.; Shin, K.; Lee, C. H. *Tetrahedron Lett.* **1996**, *37*, 197.

(64) Rexhausen, H.; Gossauer, A. *J. Chem. Soc., Chem. Commun.* **1983**, 275.

(65) Ulman, A.; Manassen, J. *J. Am. Chem. Soc.* **1975**, *97*, 6540.

(66) Fajer, J.; Borg, D. C.; Forman, A.; Dolphin, D.; Felton, R. H. *J. Am. Chem. Soc.* **1973**, *95*, 2739.

(67) Cook, M. J.; Dunn, A. J.; Howe, S. D.; Thomson, A. J.; Harrison, K. J. *J. Chem. Soc., Perkin Trans. 1* **1988**, 2453.

(68) Xie, L. Y.; Boyle, R. W.; Dolphin, D. *J. Am. Chem. Soc.* **1996**, *118*, 4853.

(69) Vogel, E. *Pure Appl. Chem.* **1996**, *68*, 1355.

(70) Kobayashi, N.; Sasaki, N.; Higashi, Y.; Osa, T. *Inorg. Chem.* **1995**, *34*, 1636.

(71) Pandian, R. P.; Chandrashekar, T. K.; Saini, G. S. S. Verma, A. L. *J. Chem. Soc., Faraday Trans.* **1993**, *89*, 677.

(72) Hill, R. L.; Gouterman, M.; Ulman, A. *Inorg. Chem.* **1982**, *21*, 1450.